Acta Crystallographica Section D
Biological Crystallography
ISSN 1399-0047

Structural basis of a novel activity of bacterial 6-pyruvoyltetrahydropterin synthase homologues distinct from mammalian 6-pyruvoyltetrahydropterin synthase activity

Kyung Hye Seo,[a]‡ Ningning Zhuang,[a] Young Shik Park,[b,c] Ki Hun Park[d] and Kon Ho Lee[a,e]*

[a]Plant Molecular Biology and Biotechnology Research Center (PMBBRC), Gyeongsang National University, Jinju 660-701, Republic of Korea, [b]School of Biological Sciences, Inje University, Kimhae 621-749, Republic of Korea, [c]Department of Health Science and Technology, Graduate School, Inje University, Kimhae 621-749, Republic of Korea, [d]Division of Applied Life Science (BK21 Plus), IALS, Gyeongsang National University, Jinju 660-701, Republic of Korea, and [e]Department of Microbiology, School of Medicine, Gyeongsang National University, Jinju 660-751, Republic of Korea

‡ Present address: Department of Functional Crops, National Institute of Crop Science, Rural Development Administration (RDA), Miryang 627-803, Republic of Korea.

Correspondence e-mail: lkh@gnu.ac.kr

Received 16 October 2013
Accepted 28 January 2014

PDB references: 6-carboxytetrahydropterin synthase, 3qn9; 3qn0; C27A mutant, complex with sepiapterin, 3qna

Escherichia coli 6-carboxytetrahydropterin synthase (eCTPS), a homologue of 6-pyruvoyltetrahydropterin synthase (PTPS), possesses a much stronger catalytic activity to cleave the side chain of sepiapterin *in vitro* compared with genuine PTPS activity and catalyzes the conversion of dihydroneopterin triphosphate to 6-carboxy-5,6,7,8-tetrahydropterin *in vivo*. Crystal structures of wild-type apo eCTPS and of a Cys27Ala mutant eCTPS complexed with sepiapterin have been determined to 2.3 and 2.5 Å resolution, respectively. The structures are highly conserved at the active site and the Zn^{2+} binding site. However, comparison of the eCTPS structures with those of mammalian PTPS homologues revealed that two specific residues, Trp51 and Phe55, that are not found in mammalian PTPS keep the substrate bound by stacking it with their side chains. Replacement of these two residues by site-directed mutagenesis to the residues Met and Leu, which are only found in mammalian PTPS, converted eCTPS to the mammalian PTPS activity. These studies confirm that these two aromatic residues in eCTPS play an essential role in stabilizing the substrate and in the specific enzyme activity that differs from the original PTPS activity. These aromatic residues Trp51 and Phe55 are a key signature of bacterial PTPS enzymes that distinguish them from mammalian PTPS homologues.

1. Introduction

6-Pyruvoyltetrahydropterin synthase (PTPS; EC 4.2.3.12) is the second enzyme in the biosynthesis of tetrahydrobiopterin (BH_4), catalyzing the conversion of dihydroneopterin triphosphate (H_2NTP) to 6-pyruvoyltetrahydropterin (PPH_4) in mammals (Thöny *et al.*, 2000; Nagatsu & Ichinose, 1999). BH_4 is a well known essential cofactor for aromatic amino-acid hydroxylases and nitric oxide synthases, which play vital roles in the biosynthesis of dopamine and serotonin in higher animals (Thöny *et al.*, 2000; Nagatsu & Ichinose, 1999). BH_4 is essential for various processes and is probably present in every cell or tissue of higher organisms. However, BH_4 is not common in bacteria, although its glycosidic forms have been found in particular species such as cyanobacteria (Chung *et al.*, 2000; Wachi *et al.*, 1995) and the anaerobic photosynthetic bacterial species from the genus *Chlorobium* (Cho *et al.*, 1998; Kang *et al.*, 1998).

A large number of PTPS homologues have been found in the genomes of many bacteria that are not known to produce BH_4 or its glycosides. These bacterial PTPS homologues can be classified into three groups depending on their activities: bacterial PTPS-I (bPTPS-I), bacterial PTPS-II (bPTPS-II) and bacterial PTPS-III (bPTPS-III) (Kong *et al.*, 2006; Pribat *et al.*,

2009). PTPS homologues belonging to bPTPS-I and bPTPS-III do not seem to be related to BH_4 synthesis, while PTPS homologues in bPTPS-II possess the genuine mammalian enzyme activity. bPTPS-I enzymes seem to have different activities from the original PTPS activity found in mammals. The PTPS homologue enzymes from *Escherichia coli* and *Synechococcus* sp. PCC 6803 have been shown to possess a peculiar catalytic activity to cleave the C6 side chain of sepiapterin to generate dihydropterin [sepiapterin side-chain releasing (SSCR) activity] *in vitro*, whereas this activity was barely detectable in human PTPS (Fig. 1; Woo *et al.*, 2002). This catalytic function of these enzymes does not suggest any comparable physiological role of the PTPS homologue enzymes from *E. coli* and *Synechococcus* sp. PCC 6803 because sepiapterin is not an indigenous metabolite. The exact functions of these bPTPS-I enzymes *in vivo* have not yet been determined. An exception is that an *E. coli* bPTPS-I homologue known as YgcM, QueD or SscR is known to be involved in queuosin biosynthesis (McCarty *et al.*, 2009) and specifically in the conversion of 7,8-dihydroneopterin triphosphate (H_2NTP) to 6-carboxy-5,6,7,8-tetrahydropterin (CPH_4) under anaerobic conditions in the bacterium, which defines the enzyme as a 6-carboxytetrahydropterin synthase (EC 4.1.2.50; eCTPS). In this reaction, sepiapterin was suggested to be involved as an intermediate in the 6-carboxytetrahydropterin synthase reaction (McCarty *et al.*, 2009).

In addition, there are other bacterial PTPS homologues that possess the same activity as the genuine PTPS enzymes in higher animals and are classified into bPTPS-II. A bacterial PTPS homologue in *Synechococcus* sp. PCC 7942 was found to have genuine PTPS activity (Kong *et al.*, 2006). When the amino-acid sequences of bPTPS-I enzymes were compared with those of bPTPS-II and mammalian enzymes, there were no distinct differences and their sequences appeared to be well conserved. Intriguingly, some of the enzymes in bPTPS-II, especially from cyanobacteria, consist of two PTPS domains organized in tandem, while the bPTPS-I enzymes have a single PTPS domain (Kong *et al.*, 2006). bPTPS-III enzymes are not related to BH_4 biosynthesis but to folate biosynthesis, in which they replace dihydroneopterin aldolase (FolB) *via* a bypass reaction (Pribat *et al.*, 2009). bPTPS-III enzymes have a glutamate instead of the conserved cysteine in PTPS in the active-site region, altering the enzymatic activity to a folate-biosynthetic enzyme differing from mammalian PTPS (Dittrich *et al.*, 2008).

Although these different bacterial PTPS homologues have recently been identified and classified, the structural basis of the different catalytic activity of the bPTPS-I class has not yet been clearly elucidated. Therefore, to understand how these bacterial PTPS homologues possess these peculiar enzyme activities with the well conserved active-site sequences observed in mammalian enzymes, we have determined the

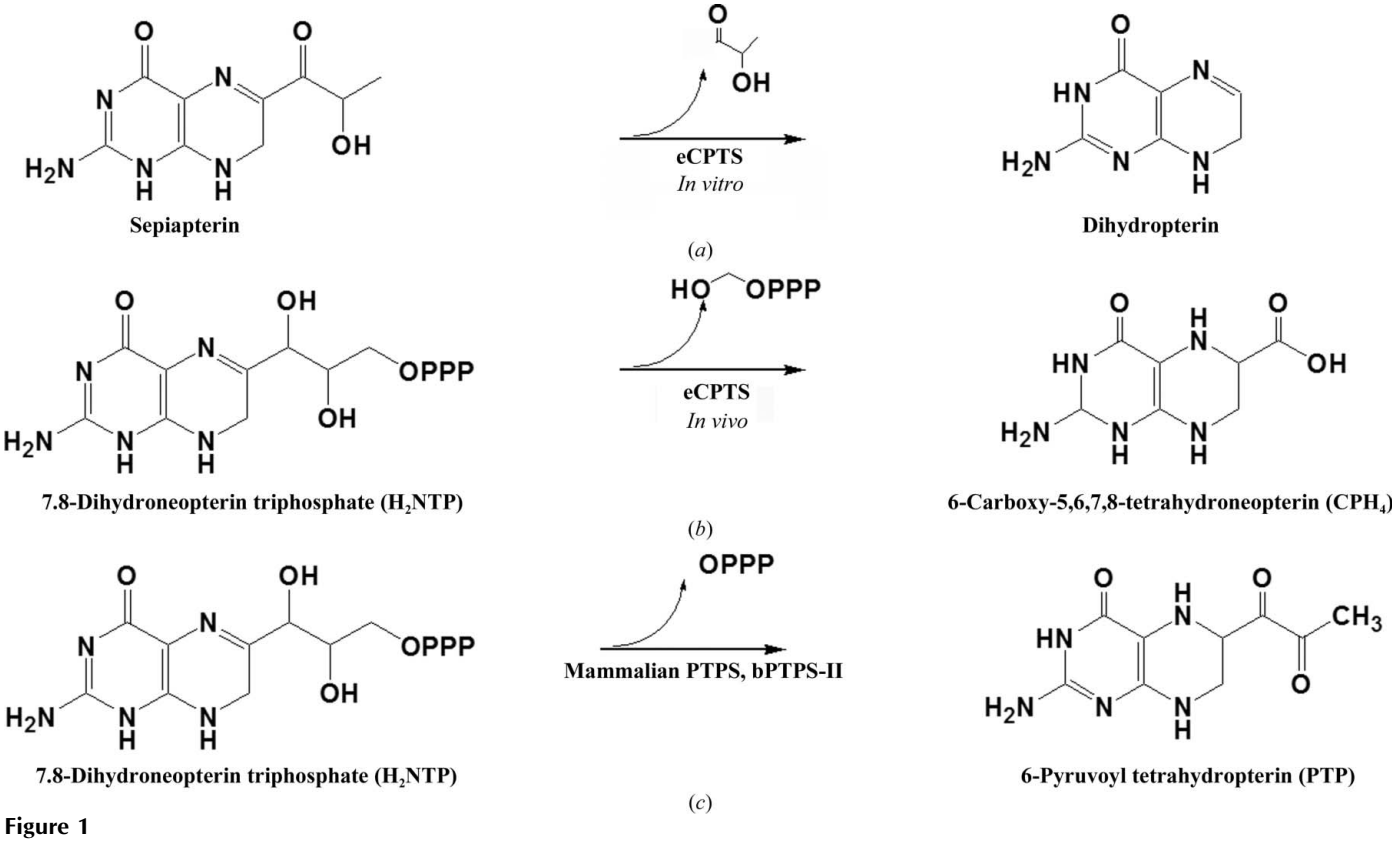

Figure 1
The enzymatic reaction of eCTPS and mammalian PTPS. (*a*) The SSCR activity of eCTPS cleaving the C6 side chain of spiapterin to dihydropterin *in vitro*. (*b*) The conversion of 7,8-dihydroneopterin triphosphate (H_2NTP) to 6-carboxy-5,6,7,8-tetrahydropterin (CPH_4) by eCTPS *in vivo* in the biosynthesis of deazapurine-containing secondary metabolites, including queuosine and toyocamycin. (*c*) Mammalian PTPS catalyses the conversion of 7,8-dihydroneopterin triphosphate (H_2NTP) to 6-pyruvoyltetrahydropterin (PPH_4) in the biosynthesis of tetrahydropterin (BH_4).

three-dimensional structures of apo eCTPS and of a Cys27Ala mutant eCTPS ($eCTPS_{C27A}$) in complex with sepiapterin and analyzed these structures in comparison with the known mammalian PTPS structures. The structures of eCTPS share the same fold as the other PTPS homologues around the catalytic and Zn^{2+} binding sites. However, two specific residues, Trp51 and Phe55, that are not found in mammalian enzymes are found to be essential for the distinct enzyme activity of eCTPS. Also, these two aromatic residues are a key signature of bacterial PTPS-I enzymes that distinguishes them from mammalian PTPS and bacterial PTPS-II enzymes. These results also provide a useful criterion for the identification of bacterial PTPS enzymes from bacterial genomes.

2. Materials and methods

2.1. Cloning, expression and purification of wild-type and mutant eCTPS proteins

eCTPS was cloned, expressed and purified as described previously (Seo *et al.*, 2008). Site-directed mutagenesis of the eCTPS gene was carried out using a Stratagene site-directed mutagenesis kit (Agilent Technologies, Santa Clara, California, USA) to mutate Cys27, Trp51, Phe55, Asp70, His71 and Glu110 to Ala, Trp55 to Phe, Trp51 to Met, Phe55 to Leu, Asp70 to Ser and Asp70 to Val. The primers for mutagenesis were designed for use with the expression vector plasmid harbouring the wild-type eCTPS DNA fragment (Supplementary Table S1[1]). The genes were amplified, inserted into pET-28b (Novagen, Madison, Wisconson, USA) and introduced into *E. coli* strain BL21(DE3). The mutant proteins were expressed and purified in a similar way as the wild-type protein. In brief, overnight starter cultures were grown at 310 K until they reached an OD_{600} of 0.6 and were induced with 0.4 m*M* IPTG for 5 h at 303 K. The cells were harvested by centrifugation and washed with phosphate-buffered saline (PBS; 8 g NaCl, 0.2 g KCl, 1.44 g Na_2HPO_4 and 0.24 g KH_2PO_4 per litre of solution, pH 7.4), resuspended in lysis buffer (50 m*M* sodium phosphate pH 8.0, 0.5 *M* NaCl, 5 m*M* imidazole) and disrupted by sonication at 277 K. After centrifugation at 277 K, the clear supernatant was filtered (Qualitative filter paper, Advantec, Japan) and applied onto a column of nickel–NTA beads (Qiagen, Hilden, Germany) pre-equilibrated with the lysis buffer. The nickel column was washed with 20 column volumes of buffer consisting of 50 m*M* Tris–HCl pH 8.0, 0.5 *M* NaCl, 30 m*M* imidazole. The protein was eluted with 50 m*M* Tris–HCl pH 8.0, 100 m*M* NaCl, 300 m*M* imidazole. The eluted protein was further purified by anion-exchange chromatography on a Source 15Q column (GE Healthcare, Piscataway, New Jersey, USA) using a ten column-volume linear gradient of 0–0.5 *M* NaCl obtained by mixing two buffers consisting of 50 m*M* Tris–HCl pH 8.0 and 50 m*M* Tris–HCl pH 8.0, 1 *M* NaCl. The eCTPS was finally purified by size-exclusion chromatography on a Superdex 200 column (GE Healthcare, Piscataway, New Jersey, USA) in PBS or in 20 m*M* Tris–HCl pH 8.0, 150 m*M* NaCl. The protein purity was examined by SDS–PAGE and native PAGE. The protein concentration was determined by the Bradford method using bovine serum albumin as a standard (Bradford, 1976). The N-terminal His tag and thrombin cleavage site were not removed for the crystallization and activity assays.

2.2. Sepiapterin side-chain releasing activity assay

The activity for the conversion of sepiapterin to 7,8-dihydropterin was measured by the disappearance of the yellow colour at 420 nm (Woo *et al.*, 2002). 50 µl reaction mixtures in PBS containing various concentrations of sepiapterin and enzyme (a total of 16 mg ml^{-1} for wild-type eCTPS and the eCTPS mutants) was prepared. The reaction was performed at 310 K for 60 min. An equal volume of cold 10% trichloroacetic acid (TCA) was added to stop the reaction, and the mixture was centrifuged at 10 000*g* for 10 min after 10 min on ice. The supernatant was diluted tenfold with distilled water and the amount of remaining sepiapterin was measured by spectral absorption at 420 nm. In order to normalize the quenching effect of TCA on the spectral absorption of sepiapterin at 420 nm, every assay was accompanied by a blank reaction without enzyme, especially when using different quantities of sepiapterin in the kinetic assay. The concentration of sepiapterin was calculated from the molar extinction coefficient (10.4 mM^{-1} cm^{-1}) at 420 nm (Matsubara *et al.*, 1966). The V_{max} and K_m values were deduced from data analysis using *GraphPad Prism* (GraphPad Software, San Diego, California, USA).

2.3. Mammalian PTPS activity

The assay of mammalian PTPS activity was performed in the absence or the presence of mouse recombinant sepiapterin reductase as described previously (Woo *et al.*, 2002). The reaction mixture consisted of 100 m*M* Tris–HCl pH 7.5, 0.1 m*M* H_2NTP, 10 m*M* $MgCl_2$, 10 m*M* DTT, 0.2 m*M* NADPH and an aliquot of the purified enzyme in a final volume of 50 µl. The mixture was incubated for 2 h at 310 K, iodine-oxidized as described by Kong *et al.* (2006) and analyzed by HPLC.

2.4. HPLC analysis of pteridines

HPLC was performed on a Kontron Model 430 equipped with a Rheodyne loop of 20 l, an Inertsil ODS-3 C18 column (5 m, 150 × 2.3 mm; GL Science, Japan) and a HP Model 1046A fluorescence detector. Pteridines were eluted isocratically with 10 m*M* sodium phosphate pH 6.0 at a flow rate of 1.2 ml min^{-1} and monitored at 350/450 nm (excitation/emission) as described previously (Woo *et al.*, 2002). Pteridine compounds were purchased from Schircks Laboratories (http://www.schircks.com).

2.5. Crystallization and data collection

The apo eCTPS protein was crystallized following a previously described protocol (Seo *et al.*, 2008). The crystal of inactive mutant $eCTPS_{C27A}$ was obtained by the hanging-drop

[1] Supporting information has been deposited in the IUCr electronic archive (Reference: MH5115).

vapour-diffusion method at 291 K in a drop consisting of 3 µl 10 mg ml^{-1} protein solution in PBS and 4 µl of a mixture of 4 µl reservoir solution (0.02 *M* $MgCl_2$, 0.1 *M* HEPES pH 7.5, 22% polyacrylic acid 5100 sodium salt) and 1 µl Index solution No. 9 (0.1 *M* bis-tris pH 5.5, 3 *M* NaCl; Hampton Research, California, USA) as an additive. To prepare crystals of the inactive mutant $eCTPS_{C27A}$ complexed with sepiapterin, the crystals were soaked with 1 m*M* sepiapterin in cryoprotectant solution (reservoir solution with 18% ethylene glycol) and incubated for 3 h before cooling in liquid nitrogen.

For data collection, the crystals were flash-cooled in liquid nitrogen. X-ray diffraction data were collected from a single rod-shaped apo eCTPS crystal (crystal form I) to 3.0 Å resolution using X-rays of wavelength 1.123 Å and a Bruker CCD detector at station 7A of the Pohang Accelerator Laboratory, Pohang, Republic of Korea. Data from needle-shaped apo eCTPS crystals (crystal form II) and $eCTPS_{C27A}$–sepiapterin complex crystals were collected to 2.3 and 2.5 Å resolution, respectively, on beamline 5C of the Pohang Accelerator Laboratory using X-rays of wavelength 1.000 Å. All diffraction images were indexed, integrated and scaled using the *HKL*-2000 suite (Otwinowski & Minor, 1997). Crystal form I of apo eCTPS belonged to the hexagonal space group *P*321, whereas crystal form II of apo eCTPS and the $eCTPS_{C27A}$–sepiapterin complex crystals belonged to the orthorhombic space group *I*222. Data-collection statistics are presented in Table 1.

Table 1
Data-collection and refinement statistics.

Values in parentheses are for the highest resolution shell.

	Wild-type eCTPS		$eCTPS_{C27A}$–sepiapterin
Data collection			
Space group	*P*321	*I*222	*I*222
Unit-cell parameters (Å)	*a* = 112.58, *b* = 112.58, *c* = 68.81	*a* = 112.76, *b* = 117.66, *c* = 153.57	*a* = 112.714, *b* = 115.882, *c* = 155.185
Wavelength (Å)	1.123	1.000	0.9999
Resolution (Å)	50.0–3.0 (3.11–3.00)	50.0–2.3 (2.42–2.34)	50–2.5 (2.54–2.50)
No. of unique reflections	10571 (1072)	43334 (4508)	35585 (1751)
Multiplicity	8.7 (2.6)	6.2 (2.7)	7.3 (7.0)
R_{merge}† (%)	23.1 (79.5)	9.4 (10.8)	6.9 (24.3)
Completeness (%)	94.8 (99.8)	99.9 (100)	99.9 (100)
$\langle I/\sigma(I)\rangle$	7.2 (5.1)	8.5 (6.5)	14.3 (12.7)
Solvent content (%)	60.95	57.61	56.34
Refinement			
Resolution (Å)	39.8–3.0	36.8–2.34	48.9–2.5
No. of reflections	10068	41012	35585
R_{work}‡/R_{free}§ (%)	19.5/26.0	22.0/27.0	18.0/22.7
R.m.s.d., bonds (Å)	0.131	0.019	0.022
R.m.s.d., angles (°)	2.021	2.054	1.916
No. of atoms			
Protein	1912	5675	5854
Ion (Zn^{2+})	2	6	6
Sepiapterin	0	0	6
Solvent	22	20	82
Ramachandran plot (%)			
Favoured regions	93.1	98.3	97.8
Allowed regions	5.6	1.6	1.9
Outliers	1.3	0.1	0.3
Average *B* factors (Å^2)			
Protein	63.96	42.2	14.35
Ion	64.73	66.67	30.41
Sepiapterin	0	0	31.09
Solvent	47.63	42.16	11.14
PDB code	3qn9	3qn0	3qna

† $R_{merge} = \sum_{hkl}\sum_i |I_i(hkl) - \langle I(hkl)\rangle| / \sum_{hkl}\sum_i I_i(hkl)$, where $\langle I(hkl)\rangle$ is the average intensity of the *i* observations. ‡ $R_{work} = \sum_{hkl} ||F_{obs}| - |F_{calc}|| / \sum_{hkl} |F_{obs}|$. R_{work} is calculated with the 95% of the reflections used for structure refinement. § R_{free} is calculated using the remaining 5% of reflections that were randomly selected and excluded from refinement.

2.6. Model building and refinement

Initially, molecular replacement was attempted with the high-resolution data from crystal form II of apo eCTPS using the *Pseudomonas aeruginosa* PTPS homologue (PDB entry 2oba; T. W. McGrath, G. Kisselman, K. Battaile, V. Romanov, J. Wu-Brown, J. Guthrie, C. Virag, K. Mansoury, A. M. Edwards, E. F. Pai & N. Y. Chirgadze, unpublished work; 69% sequence identity) as a search model. However, this was unsuccessful because of an ambiguity in the space group, which could be either *I*222 or $I2_12_12_1$. Therefore, to determine the space group and structure of crystal form II of apo eCTPS, the data fror crystal form I of apo eCTPS in space group *P*321 were first used for molecular replacement and the structure was solved using the program *AMoRe* (Navaza, 1994) in the *CCP*4 suite (Winn *et al.*, 2011) with the *P. aeruginosa* PTPS homologue as a search model. The structure of the apo-eCTPS in crystal form II was determined by molecular replacement with the model of crystal form I of apo-eCTPS in space group *P*321 as a search model using the program *MOLREP* (Vagin & Teplyakov, 2010) in the *CCP*4 suite (Winn *et al.*, 2011). The initial structure refinement was carried out with *CNS* (Brünger *et al.*, 1998) and the final stage of the refinement was carried out with *REFMAC* (Murshudov *et al.*, 2011). The residues were modelled by several cycles of manual building using the graphics program *O* (Jones *et al.*, 1991) and *Coot* (Emsley & Cowtan, 2010). The structure of the $eCTPS_{C27A}$–sepiapterin complex was determined by molecular replacement using *MOLREP* in the *CCP*4 suite with the wild-type apo eCTPS structure from crystal form II as a search model, and was refined and built manually in the same way as apo eCTPS. The stereochemistry of the final models was examined by *PROCHECK* (Laskowski *et al.*, 1993) in the *CCP*4 suite. Detailed refinement statistics are summarized in Table 1. All figures were produced using *PyMOL* (http://www.pymol.org). *DaliLite* (Holm & Park, 2000) was used for pairwise structure alignment and comparison. Sequence alignment was performed with *ClustalW* (Larkin *et al.*, 2007).

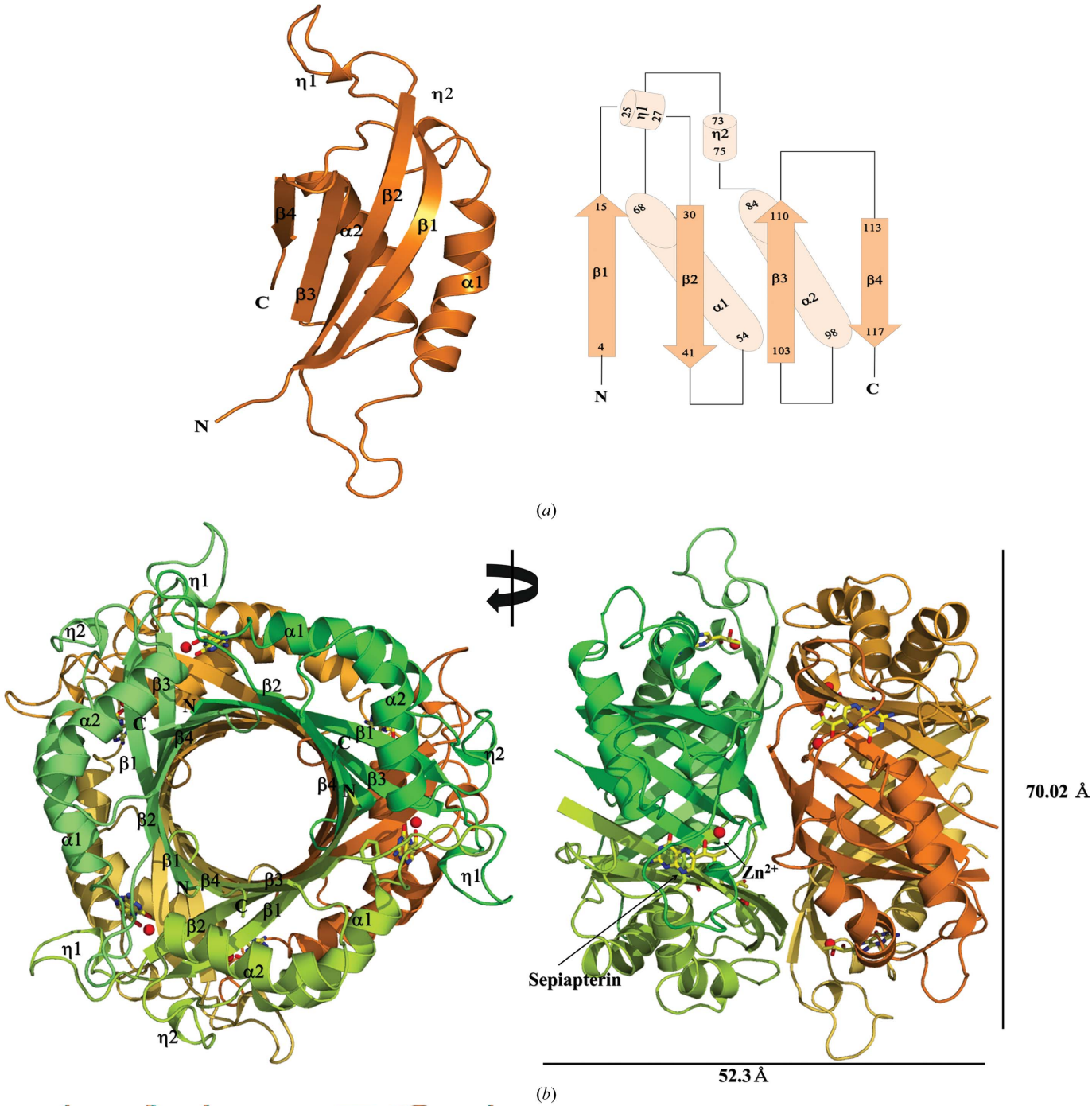

Figure 2
Crystal structure of eCTPS. (*a*) A ribbon representation and topology of the monomer structure. (*b*) A ribbon representation of the hexameric structure of eCTPS viewed from the top (left) and the side (right) of the hexamer. β-Strands and α-helices are labelled in numerical order from the N-terminus. Sepiapterin (oxygen, red; carbon, yellow; nitrogen, blue) is shown in stick representation. Zn^{2+} ions are represented as red spheres. (*c*) Superposition of apo eCTPS (green) and the $eCTPS_{C27A}$–sepiapterin complex (orange). The side chain of Trp51 in the complex (carbon, orange; nitrogen, blue; oxygen, red) is rotated from its position in apo eCTPS (carbon, green, nitrogen, blue; oxygen, red) by about 180° around the $C^{\alpha}-C^{\beta}$ bond. The main chain of Phe55 moves about 1.6 Å closer to sepiapterin (marked with a black dotted arrow). The movement of the side chain is marked with a red arrow showing ~180° rotation.

3. Results

3.1. Overall structure of eCTPS

We solved the structures of two different constructs of full-length 6-carboxytetrahydropterin synthase from *E. coli* (eCTPS; 121 residues): wild-type eCTPS (apo eCTPS) and eCTPS with a mutation of the catalytic nucleophile Cys27 to alanine ($eCTPS_{C27A}$) in complex with sepiapterin. The electron density for sepiapterin in the complex was well defined (Fig. 3). In the crystal, eCTPS formed a hexamer consisting of two closely interacting trimers in the asymmetric unit, although it existed as trimers and dodecamers in solution, as confirmed by gel-filtration chromatography and a chemical cross-linking experiment (Supplementary Fig. S1). Each monomer folds into a single domain with two α-helices, two short α-helices and four β-sheets, $\beta1\uparrow\beta2\downarrow\beta3\uparrow\beta4\downarrow$, with all strands exhibiting an antiparallel pattern (Fig. 2*a*). The hexamer of eCTPS comprised a central β-barrel surrounded by α-helices. The overall diameter of the trimer was 70.02 Å, and the hexamer was 52.3 Å in length along the threefold axis (Fig. 2*b*). The active sites were located at the interfaces between trimers. The structure of apo eCTPS was almost identical to that of the $eCTPS_{C27A}$–sepiapterin complex, with a root-mean-square deviation (r.m.s.d.) of 0.556 Å for all C^{α} atoms. There is one Zn^{2+} ion bound in each monomer. The positions of the catalytic triad and the residues coordinating to the bound Zn^{2+} ion were well conserved in the structures of apo eCTPS and the $eCTPS_{C27A}$–sepiapterin complex. However, the $\alpha1$ helix (residues Ile52–Pro64) in the complex is positioned closer to the sepiapterin by 1.6 Å compared with the apo form. A conformational change of the side chain of residue Trp51 was observed upon substrate binding (Fig. 2*c*). The side chain of Trp51 rotates 180° around the $C^{\alpha}-C^{\beta}$ bond for substrate binding. The side chain of Trp51 rotates towards the pterin ring of the bound sepiapterin and fixes the ring through stacking interactions together with the side chain of Phe55.

3.2. Sepiapterin and Zn^{2+} bound in the active site

In the $eCTPS_{C27A}$–sepiapterin complex structure, the active sites can be identified from the bound sepiapterin molecules and Zn^{2+} ions. The active sites of eCTPS are located at the interfaces of three monomers. The interface is constructed by two chains (*A* and *B*) from one trimer and one chain (*D*) from the other trimer (Fig. 3). eCTPS contains an intersubunit catalytic triad motif composed of amino-acid residues Cys27 from chain *A* and Asp70 and His71 from chain *D*. The residues of the catalytic triad activate the nucleophile Cys27 as a proton donor. Asp70 and His71 from chain *D* are closely positioned, with bond lengths of 3.16 and 3.20 Å between N^{δ} of the polarized His71 and $O^{\gamma1}$ and $O^{\gamma2}$ of the carboxyl group of Asp70, respectively. The sepiapterin binds into the cleft formed by chains *A* and *B*. The sepiapterin is bound through hydrogen bonds formed between N1 and N8 of the pterin ring and the O^{γ} atom of Asp54 in chain *B*, between N2 and the backbone carbonyl O atom of Ile53 in chain *B* and through a salt bridge between the N2 and N3 atoms of the pterin ring and the side chain of Glu86 in chain *A*. The side chain of Glu110 in chain *A* is close to N5 of the pterin ring and O9 of

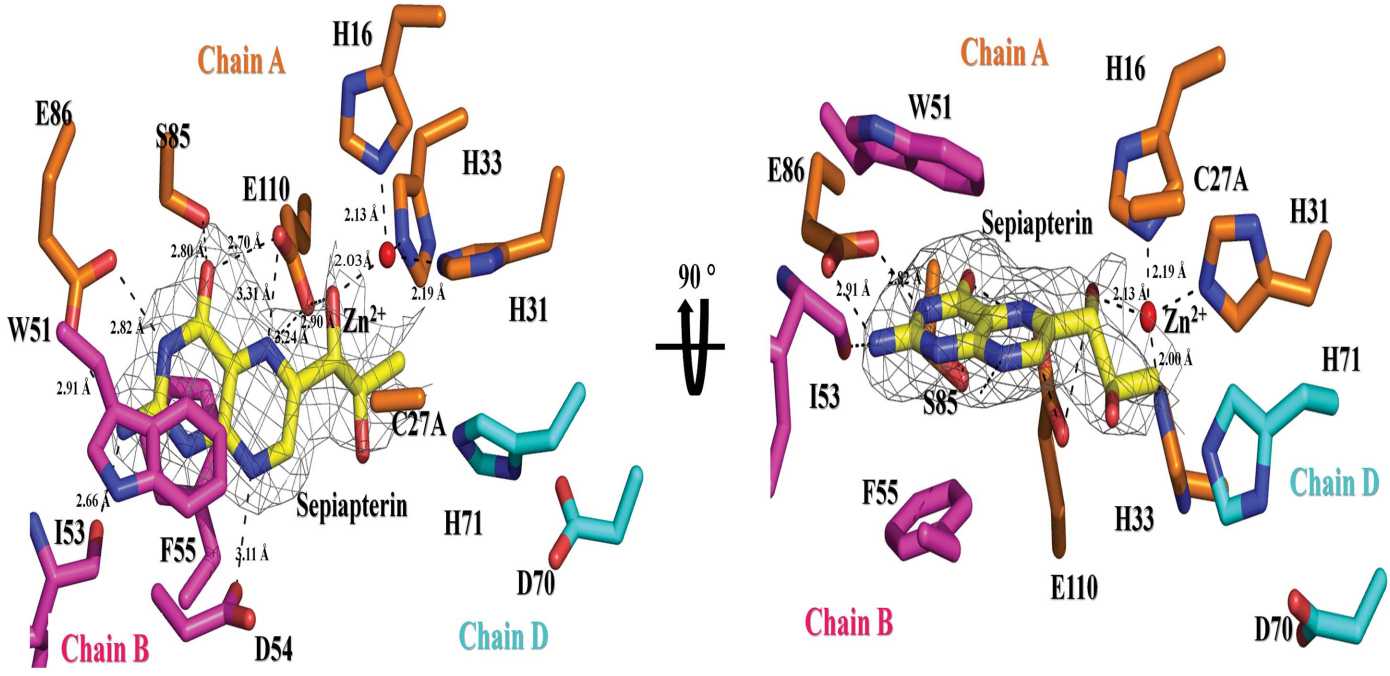

Figure 3
Sepiapterin and Zn^{2+} ion bound in the active site of eCTPS. The hydrogen-bond interactions between sepiapterin (C atoms, yellow; N atoms, blue; O atoms, red) and side chains are represented by dashed lines with distances marked. A view rotated by 90° about the *x* axis from the left figure is shown in the right figure. The pterin ring of the bound sepiapterin is stacked between Trp51 and Phe55. Residues from chain *A*, chain *B* and chain *D* are coloured with C atoms in orange, magenta and cyan, respectively, N atoms in blue and O atoms in red. The $2F_o - F_c$ electron-density map of sepiapterin in the $eCTPS_{C27A}$–sepiapterin complex structure contoured at 3σ (grey) clearly shows the position of sepiapterin. A Zn^{2+} ion is represented as a red sphere.

the sepiapterin side chain, providing a possible additional proton source. In particular, the pterin ring of the sepiapterin is stacked between Trp51 and Phe55 from chain *B*, with stacking distances of about 4.11 and 3.55 Å, respectively.

There is one Zn^{2+} ion bound in each monomer. The Zn^{2+} ion is coordinated to the N^{ε} atoms of the side chains of His16, His31 and His33, with distances of 2.13, 2.19 and 2.00 Å, respectively, and the side chain of Cys27, which are all present in the same monomer chain (Fig. 3). In the complex structure, the Zn^{2+} ion is coordinated by the O atom (O9) of the sepiapterin side chain with a distance of 2.03 Å. O9 is in the *trans* conformation to O10 (the torsion angle O9—C9—C10—O10 is 107.96°). In this conformation, O9 is directed towards the Zn^{2+} ion. These Zn^{2+}-binding residues and the O atom in sepiapterin contribute to bind the Zn^{2+} with a coordination sphere with a tetrahedral geometry.

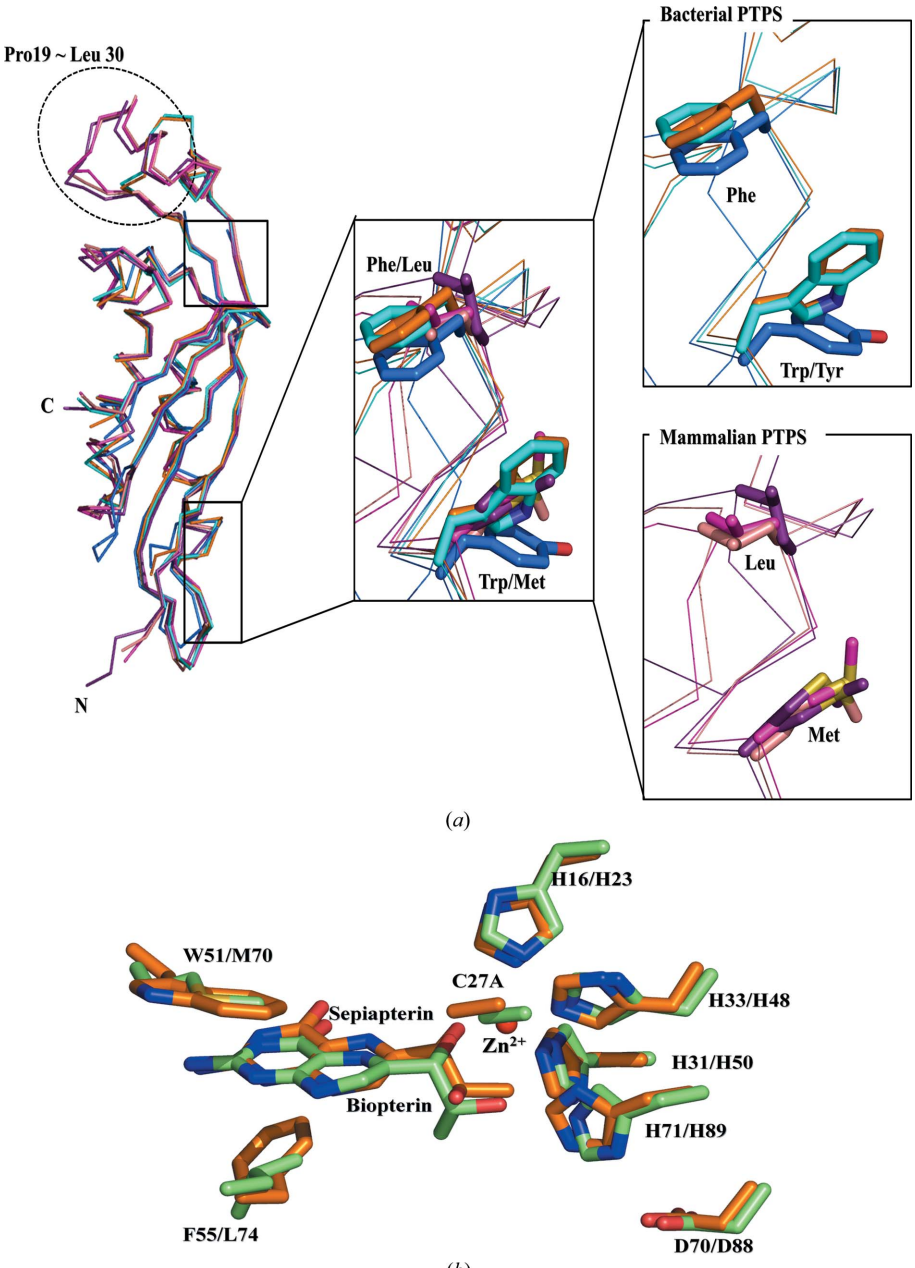

Figure 4
Superposition of structures of bacterial PTPS homologues and mammalian PTPSs. (*a*) Structures of PTPS homologues were superposed: bacterial PTPS homologues from *E. coli* with sepiapterin (PDB entry 3qna, orange), *P. aeruginosa* (PDB entry 2oba, cyan) and *P. horikoshii* OT3 (PDB entry 2dj6, blue), mammalian PTPS enzymes from rat with biopterin (PDB entry 1b66, magenta) and human (PDB entry 3l2b, pink) and a nematode PTPS enzyme from *C. elegans* (PDB entry 2g64, purple). The boxes show details of the active site. Enlargements present the side chains of residues involved in the binding of the substrate among the PTPS homologues. The residues Met and Leu of mammalian PTPS and Trp and Phe of bacterial PTPS homologues superposed well. Two aromatic residues Trp and Phe stacking the substrate in bacterial PTPS structures were superimposed, which shows that these two residues are well conserved in the structures of bacterial PTPS. (*b*) Superposition of the $eCTPS_{C27A}$–sepiapterin complex (orange) with the rat PTPS–biopterin complex (green) in the active site.

3.3. Structural comparison of eCTPS with other bacterial and mammalian PTPS homologues

Amino-acid sequence comparisons using a *BLAST* search of the NCBI database (http://blast.ncbi.nlm.nih.gov) revealed that bacterial PTPS homologues and mammalian PTPS enzymes share greater than 30% similarity (Fig. 4*c*). The *E. coli* 6-carboxytetrahydropterin synthase (eCTPS) shares high sequence identities with human PTPS (27% identity) and rat PTPS (26% identity), with well conserved active-site residues Cys27 and His71 (corresponding to Cys42 and His90 used for the conversion of H_2NTP to PPH_4 in the human enzyme; Ploom *et al.*, 1999). A search for structural homologues using the *DALI* server (Holm & Sander, 1995) identified a set of PTPS homologue proteins from bacteria and mammals, including PTPS homologue proteins from *P. aeruginosa* (PDB entry 2oba; *Z*-score 21.7), *Pyrococcus horikoshii* OT3 (PDB entry 2dj6; *Z*-score 16.1; RIKEN Structural Genomics/Proteomics Initiative, unpublished work), *Caenorhabditis elegans* (PDB entry 2g64; *Z*-score 17.3; New York SGX Research Center for Structural Genomics, unpublished work), human (PDB entry 3i2b; *Z*-score 17.3; Structural Genomics Consortium, unpublished work) and rat (PDB entry 1b66; *Z*-score 17.2; Ploom *et al.*, 1999; Nar *et al.*, 1994), with *Z*-scores greater than 17.2. The structure of eCTPS shares the same fold as the other PTPS homologues around the catalytic and Zn^{2+} binding sites, with r.m.s.d.s of 0.5–1.8 Å. PTPS proteins also have a well conserved Ser/Thr-Glu motif (Ser86 and

Glu87 in eCTPS, Thr106 and Glu107 in rat) that forms hydrogen bonds to the pyrimidine ring (Lawrence *et al.*, 2006). Comparisons of the structures of eCTPS with those of human and rat PTPS show that the loop between β1 and β2 (residues Pro19–Leu30 in eCTPS) is shorter than those in rat PTPS (residues His26–Gly47) and in human PTPS (residues His27–Gly48) (Fig. 4*a*). This seems to be owing to low sequence similarity among these enzymes in this loop region.

When the sepiapterin binding site in the $eCTPS_{C27A}$–sepiapterin complex structure was compared with that in the rat PTPS structures, the bound sepiapterin and biopterin in both the structures was positioned at almost same site with similar conformations except for the end of the side chain (Fig. 4*b*). The sepiapterin bound to $eCTPS_{C27A}$ was stacked between the aromatic side chains of Trp51 and Phe55, while the biopterin in the rat PTPS complex was bound by hydrogen bonds to Met70. The residues Trp51 and Phe55 in eCTPS corresponded to Met70 and Leu74 in rat PTPS when the amino-acid sequences were aligned (Fig. 4*c*). Interestingly, it was found from the sequence alignment that Trp or Phe residues are not found in the corresponding positions in the sequences of mammalian PTPS proteins.

3.4. Identification of the residues essential for the unusual activity of bacterial PTPS homologues

To examine which residues in eCTPS are critical for the unusual activity of bacterial PTPS, the residues involved in catalysis and substrate binding were mutated by site-directed mutagenesis. The catalytic triad residues Cys27, Asp70 and His71 were replaced by alanine, and Asp70 was additionally mutated to valine. Trp51, Phe55 and Glu110, which were found to be involved in sepiapterin binding, were also chosen for mutation. Specifically, Trp51 was mutated to alanine, phenylalanine and methionine, Phe55 to alanine and leucine, and Glu110 to alanine. Among the mutations, no soluble mutant eCTPS proteins were obtained using the D70A, W51A and D70S mutations, which indicates that mutation of these residues might lead to structural instability.

The mutant eCTPS proteins generally showed decreased sepiapterin side-chain releasing (SSCR) activity compared with the wild type (Table 2). A significant decrease in the bacterial PTPS (SSCR) activity was observed for the C27A, W55A, H71A, E110A and D70V mutants. The C27A mutant had a 15-fold higher affinity (K_m), a 13-fold lower turnover number (k_{cat}) and a 13-fold reduced V_{max} value of 7.80 $\pm$ 0.34 nmol min^{-1} mg^{-1} compared with wild-type eCTPS (Table 2). The SSCR activities of mutants with H71A and D70V mutations decreased by fourfold to tenfold. The mutation of Glu110, which interacts with the side chain and the pterin ring of the sepiapterin, resulted in the largest decrease (13-fold) among the alanine mutants, which suggests that Glu110 is another essential residue in catalysis in addition to Cys27. Interestingly, the C27A, F55A, H71A, E110A and D70V mutants in which residues are replaced by the smaller residues alanine and valine had lower affinity (K_m) values and

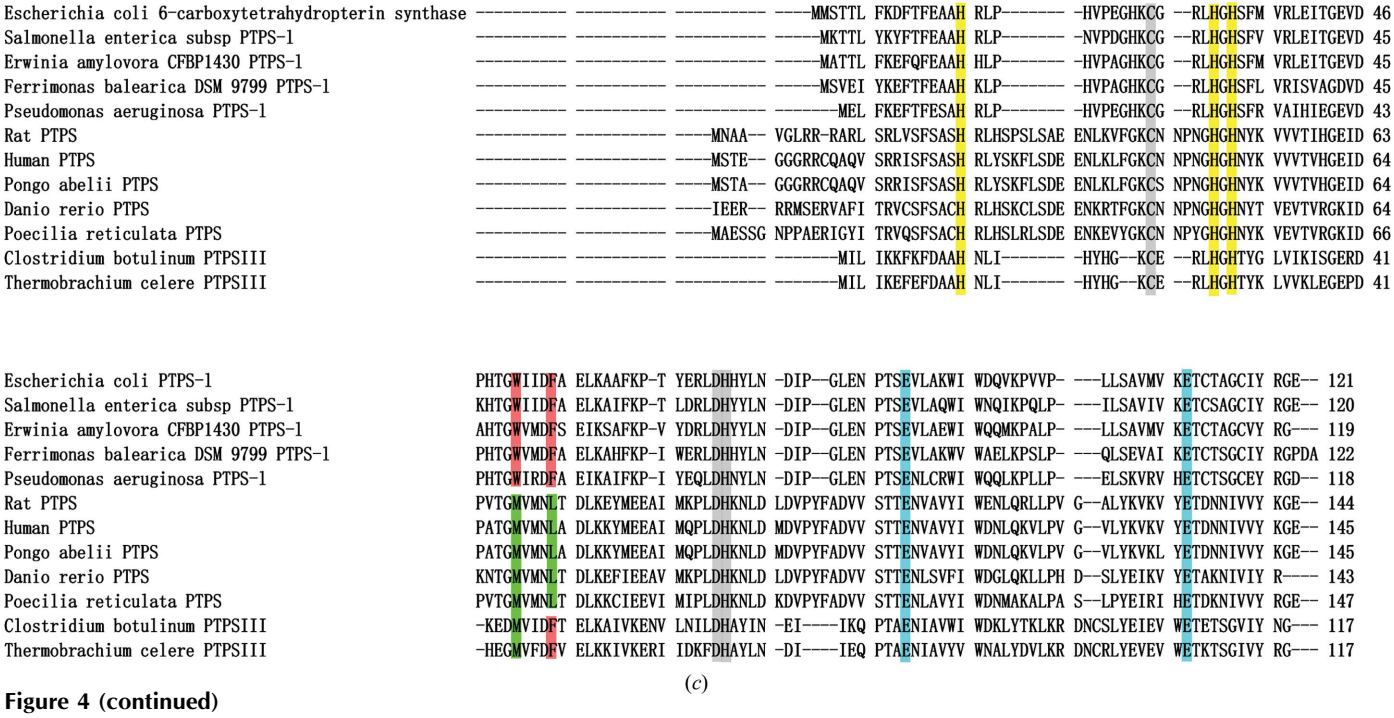

(*c*)

Figure 4 (continued)

(*c*) Sequence alignment of bacterial and mammalian PTPS homologues. The amino-acid sequences of PTPS homologues from bacteria and eukaryotes including mammals were aligned with that of eCTPS. The names of the organisms are presented to the left of the sequences. The absolutely conserved residues are His16, His31 and His33 (yellow box) and Cys27 (grey box) for Zn^{2+} ion binding, Cys27, Asp71 and His72 (grey box) forming the catalytic triad, and Glu85 and Glu110 (blue box) for hydrogen-bond interaction with the substrate. The bacterial PTPS-I enzymes have a conserved Trp51 and Phe55 (red box) which bind the pterin ring of the substrate. However, mammalian PTPSs and bacterial PTPS-II enzymes have a well conserved Met and Leu (green box) at the same positions.

Table 2
The SSCR activities of wild-type eCTPS and its mutants.

The activities were determined under the standard assay conditions using varying concentrations of sepiapterin.

Bacterial PTPS-I	V_{max} (nmol min^{-1} mg^{-1})	K_m (mM)	k_{cat} (min^{-1})	k_{cat}/K_m (M^{-1} s^{-1})
Escherichia coli				
Wild type	104.6 ± 7.17	1.80 ± 0.13	4.33 ± 0.29	14.4×10^4
C27A	7.80 ± 0.19	0.12 ± 0.01	0.32 ± 0.008	16.6×10^4
F55A	51.42 ± 0.63	0.87 ± 0.01	2.13 ± 0.026	37.1×10^4
H71A	22.34 ± 2.33	0.84 ± 0.10	0.92 ± 0.096	14.7×10^4
E110A	7.50 ± 0.45	0.16 ± 0.02	0.31 ± 0.02	6.7×10^4
D70V	9.75 ± 0.98	0.25 ± 0.06	0.40 ± 0.04	11.8×10^4
W51F	355.06 ± 6.63	2.50 ± 0.39	14.69 ± 0.27	10.6×10^4
W51M	23.02 ± 0.70	4.31 ± 0.28	0.95 ± 0.03	1.32×10^4
F55L	3.39 ± 0.07	1.07 ± 0.06	0.14 ± 0.003	0.78×10^4
W51M and F55L	42.44 ± 0.43	7.67 ± 0.13	1.76 ± 0.02	1.38×10^4
Pseudomonas aeruginosa	8.01 ± 0.12	0.09 ± 0.004	0.33 ± 0.005	22.2×10^4
Shigella boydii	8.79 ± 0.18	0.16 ± 0.007	0.36 ± 0.007	13.6×10^4

reduced turnover numbers (k_{cat}), which indicate tighter binding but a much lower turnover rate. On the other hand, the W51F, W51M and F55L mutants with mutations to the relatively larger residues Phe, Met and Leu had similar or higher K_m values, implying less tight binding than the wild type. These differences in the binding affinity among the mutants seem to be associated with the size of residues in the binding site. Those mutants with smaller residues seem to have a larger binding surface than the mutants with larger residues, resulting in tighter binding. However, all of the mutants except the W51F mutant showed greatly reduced turnover numbers, which suggests that although these mutants bind more tightly their reaction rates are much lower than that of the wild type, resulting in decreased SSCR activities. These low SSCR activities arising from the mutation of active-site residues confirm the importance of these residues in catalysis. Specifically, when Phe55 was mutated to Leu, the SSCR activity decreased by about 30-fold. Furthermore, surprisingly, when Trp51 was replaced by phenylalanine V_{max} and k_{cat} increased by about threefold compared with those of the wild type, resulting in an unexpected increase in SSCR activity. The stacking interactions mediated by two Phe residues seem to provide a more favourable environment for increased SSCR activity than other residues through π-electron polarization. Also, the W51F mutant showed a similar catalytic efficiency (k_{cat}/K_m) to the wild type, while the catalytic efficiencies of the W51M, W51L and F55L mutants were reduced more than tenfold. These results indicate that the stacking interactions mediated by the side chains of Trp51 and Phe55 are of great importance for the unusual activity of eCTPS.

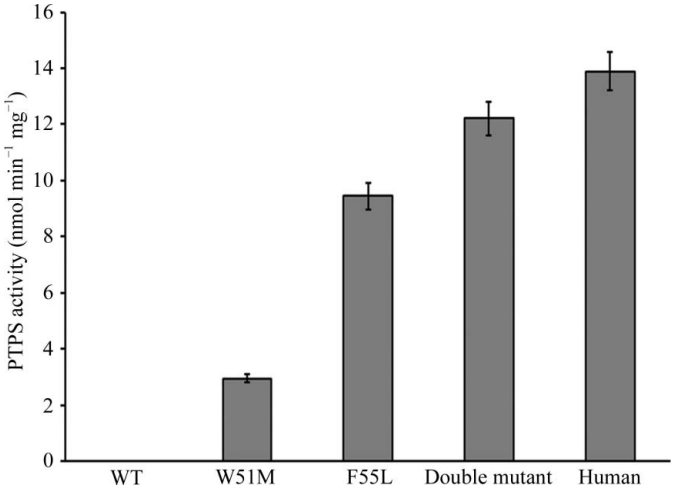

Figure 5
PTPS activity of eCTPS mutants. The PTPS activities of wild-type eCTPS, the W51M and F55L single mutants, the W51M and F55L double mutant and the human PTPS enzyme were measured by the synthesis of BH_4 in a coupled assay with sepiapterin reductase. All enzymatic activity values are expressed as a mean ± SD obtained from three independent experiments.

3.5. Conversion of the activity of eCTPS to mammalian PTPS activity

The residues Trp51 and Phe55 critical for the novel activity of eCTPS are not found in mammalian PTPS homologues. Therefore, the residues Trp51 and Phe55 of eCTPS were mutated to the corresponding residues Met and Leu in mammalian PTPSs to determine whether bacterial PTPS could have mammalian PTPS activity (Fig. 4*b*). Wild-type eCTPS has a negligible mammalian PTPS activity (Fig. 5). However, when Trp51 and Phe55 were mutated to the Met and Leu present in mammalian PTPS enzymes (single-residue mutants) or both of the residues were replaced by Met and Leu (double mutant), these mutants had mammalian PTPS activities comparable to the mammalian enzymes but had much lower bacterial PTPS (SSCR) activities than wild-type eCTPS. In particular, the mammalian PTPS activities of the F55L single mutant (9.45 ± 0.34 nmol min^{-1} mg^{-1}) and double mutant (12.2 ± 0.5 nmol min^{-1} mg^{-1}) were very similar to the activity of human PTPS protein (13.89 ± 0.45 nmol min^{-1} mg^{-1}), while the W51M mutant exhibited a weaker mammalian PTPS activity (Fig. 5). Unexpectedly, this F55L mutation alone restored most of the mammalian PTPS activity (about 70% of that of the human enzyme). These results suggest that the Trp51 and Phe55 residues are essential for the SSCR activity and that Phe55 is a key residue that determines the differing bacterial enzyme activity from the mammalian PTPS activity.

4. Discussion

PTPS is the second enzyme in the conversion of H_2NTP in tetrahydropterin biosynthesis in mammals (Thöny *et al.*, 2000). In prokaryotes, many proteins have been found to be mammalian PTPS homologues. These PTPS homologues can be classified into three groups depending on their specific

activities. One group of bacterial PTPS homologues (bPTPS-I) has a novel enzyme activity (6-carboxytetrahydropterin synthase activity) that differs from the mammalian PTPS activity, while the other group of bacterial PTPS homologues (bPTPS-II) possess the same PTPS activity as mammalian PTPS (Fig. 6). Although the bPTPS-II and mammalian PTPS enzymes have the same enzyme activity involved in BH_4 biosynthesis, their domain organizations are different. Mammalian PTPS enzymes have one PTPS domain and exist as a hexamer in solution, but the bPTPS-II proteins consist of two PTPS domains organized in tandem and form a trimer as a functional unit in solution. Bacterial PTPS-III homologues do not possess the original PTPS activity but have the activity of converting dihydronepterin to 6-hydroxymethyldihydropterin (HMDHP) in the classical folate-biosynthesis pathway (Dittrich *et al.*, 2008; Pribat *et al.*, 2009).

It has previously been reported that a PTPS homologue in *E. coli* showed the unusual activity of converting sepiapterin to dihydropterin (Woo *et al.*, 2002) *in vitro* and H_2NTP to CPH_4 under anaerobic conditions *in vivo*, which defined the *E. coli* enzyme as a 6-carboxytetrahydropterin synthase (eCTPS; McCarty *et al.*, 2009). However, it was not clear why the enzyme activity of eCTPS differs from that of PTPS of mammals, as eCTPS and mammalian PTPS homologues share high amino-acid sequence identities with well conserved active-site triads. To better understand the peculiar activity of eCTPS and to elucidate the structural elements that define the bacterial PTPS enzymes, we have determined crystal structures of eCTPS and performed biochemical and mutational studies.

The crystal structures of apo eCTPS and the $eCTPS_{C27A}$–sepiapterin complex were similar but there was a subtle change in the substrate-binding site. The sepiapterin in the complex structure was bound between the side chains of two aromatic residues Trp51 and Phe55. In the complex the side chain of Trp51 is rotated about 180° from the position in the apo structure towards the pteridine ring of the bound sepiapterin and fixes the sepiapterin in position through stacking interactions together with the side chain of Phe55 (Figs. 2*c* and 3).

It has previously been suggested that sepiapterin is an intermediate in the carboxytetrahydropterin synthase reaction from H_2NTP to 6-carboxytetrahydropterin, in which sepiapterin is converted to 6-carboxytetrahydropterin by an aldolase-like mechanism and subsequent tautomerization (McCarty *et al.*, 2009). Intriguingly, the sepiapterin side chain is cleaved completely by eCTPS to generate dihydropterin *in vitro*, whereas this activity was barely detectable in human PTPS (Woo *et al.*, 2002). The crystal structure of the $eCTPS_{C27A}$–sepiapterin complex provides insight into the reaction mechanism of the SSCR activity. It seems that the sepiapterin side chain is cleaved in a cysteine protease-like mechanism involving the nucleophile Cys27, which is one of the catalytic triad residues (Cys27, Asp70 and His71), together with a Zn^{2+} ion and Glu110 for stabilization of the intermediate, followed by tautomerization to generate dihydropterin (Supplementary Fig. S2). For this reaction, Glu110 was confirmed to be important from the site-directed mutagenesis in addition to the catalytic triad of the eCTPS enzyme.

In addition, when compared with mammalian PTPS structures in the PDB, the structures of eCTPS showed a similar overall folding. However, distinct structural differences between eCTPS and mammalian PTPS are observed around the substrate-binding site, especially at residues Trp51 and Phe55 in eCTPS. As described above, the Trp51 and Phe55 residues fix the pterin ring of the substrate in position by stacking it between their side chains. Analysis of the primary sequences of PTPS homologues in bacteria and mammals reveals that Trp51 and Phe55 are only well conserved in some of the bacterial PTPS homologues and are not conserved at all in mammalian PTPS (Figs. 4*a*, 4*b* and 4*c*). The residues Trp51 and Phe55 in eCTPS correspond to Met70 and Leu74 in the rat enzyme and Met69 and Leu73 in the human enzyme (Figs. 4*a* and 4*b*). The Met residue is well conserved in mammalian

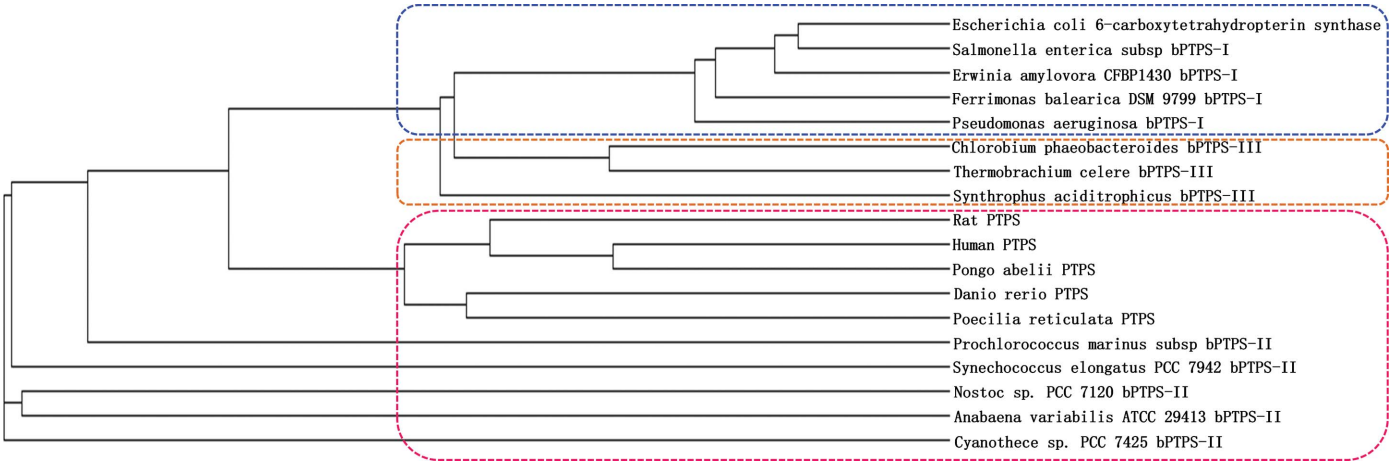

Figure 6
Phylogenetic tree of PTPS proteins. The multiple alignments were made using the Neighbour Joining phylogenetic tree in *BioEdit* (Hall, 1999). Homologous proteins of bPTPS-I, bPTPS-II, bPTPS-III and mammalian PTPS were searched for using a *BLAST* search of the NCBI database (http://blast.ncbi.nlm.nih.gov) using eCTPS and human PTPS. Mammalian PTPS and bPTPS-II are marked with a red dashed line, bPTPS-I with a blue dashed line and bPTPS-III with an orange dashed line.

PTPS enzymes and has been shown to make interactions with the substrate in the rat PTPS structure (Nar *et al.*, 1994; Ploom *et al.*, 1999), while the Leu residue is not conserved and is not involved in substrate binding. To examine the specific roles of the two aromatic residues in the unusual activity of eCTPS, the Trp51 and Phe55 residues of eCTPS were mutated to the corresponding residues Met and Leu in mammalian PTPS. Before these mutations, the wild-type eCTPS had negligible mammalian PTPS activity. Interestingly, eCTPS with these mutations had the mammalian PTPS enzyme activity but had negligible bacterial PTPS activity (Fig. 5). Most of the mammalian PTPS activity was restored by the F55L mutation alone. Therefore, these results suggest that Trp51 and Phe55, which are not found in mammalian PTPS, are essential for the novel activity of eCTPS, and specifically that Phe55 is a key residue in determining the unusual bacterial enzyme activity. Also, this is the first experiment in which a mutation has been shown to convert the specific activity of an enzyme to another enzyme activity different from the original activity.

From the sequence database search, many other PTPS homologues in bacteria have been found to have two aromatic residues corresponding to Trp51 and Phe55 of eCTPS (Fig. 4*c*). To determine whether they have unusual activity like eCTPS, recombinant bPTPS-I homologue proteins from *P. aeruginosa* and *Shigella boydii* were produced and their SSCR activities were examined. Intriguingly, it was found that they have SSCR activity like eCTPS (Table 2). Consequently, this confirms that PTPS homologues in bacteria that contain Trp51 and Phe55 possess this unusual enzyme activity that differs from the genuine mammalian PTPS activity. In contrast, some PTPS homologues in bacteria that possesses the original mammalian activity, belonging to bPTPS-II, have Met and/or Leu residues instead of Trp and Phe around the active site (Fig. 4*c*).

PTPS homologues in bacteria are classified by their enzyme activities: bPTPS-I, bPTPS-II and bPTPS-III. Intriguingly, the activities of the bPTPS-I proteins are highly correlated with the amino-acid sequence around the substrate-binding site. Amino-acid sequence analysis and a mutagenesis study of eCTPS show that all of the bPTPS-I homologues have two aromatic residues Trp and Phe (Trp51 and Phe55 in eCTPS) and that the bPTPS-II homologues do not have these two aromatic residues but have Met and/or Leu at the pterin binding site. In addition, bPTPS-III homologues have Met instead of Trp at the pterin binding site (Fig. 4*c*). These results suggest that the Trp and Phe residues in bPTPS-I (Trp51 and Phe55 in eCTPS) are essential in determining the enzymatic properties of the bPTPS-I proteins. Therefore, the presence of these two aromatic residues defines bPTPS-I as a 6-carboxytetrahydropterin synthase and can be used as an indicator to distinguish bPTPS-I proteins from mammalian PTPS, bPTPS-II and bPTPS-III among the PTPS homologues.

In conclusion, from detailed three-dimensional structures of eCTPS and through mutational and biochemical analyses we have found that the two aromatic residues Trp and Phe in the substrate-binding site (Trp51 and Phe55 in eCTPS) are the key residues for the novel activity (6-carboxytetrahydropterin synthase activity) of the bPTPS-I proteins in bacteria and are an essential determinant that distinguishes bPTPS-I enzymes from mammalian PTPS, bPTPS-II and bPTPS-III enzymes. These results provide a deeper understanding of the essential signature of bacterial PTPS-I enzymes responsible for their extraordinary enzyme activity, which differs that from that of the mammalian enzymes within a well conserved overall structure.

We thank the staff at beamlines 5C and 7A of Pohang Accelerator Laboratory for help with data collection. This work was supported in part by National Science Foundation grants NRF-2012R1A1A2044394 (KHL), NRF-2012M1A2A2671832 (KHL) and NRF-2013M3A9A6003180 (KHP) funded by the Korean government.

References

Bradford, M. M. (1976). *Anal. Biochem.* **72**, 248–254.
Brünger, A. T., Adams, P. D., Clore, G. M., DeLano, W. L., Gros, P., Grosse-Kunstleve, R. W., Jiang, J.-S., Kuszewski, J., Nilges, M., Pannu, N. S., Read, R. J., Rice, L. M., Simonson, T. & Warren, G. L. (1998). *Acta Cryst.* D**54**, 905–921.
Cho, S.-H., Na, J.-U., Youn, H., Hwang, C.-S., Lee, C.-H. & Kang, S.-O. (1998). *Biochim. Biophys. Acta*, **1379**, 53–60.
Chung, H. J., Kim, Y.-A., Kim, Y. J., Choi, Y. K., Hwang, Y. K. & Park, Y. S. (2000). *Biochim. Biophys. Acta*, **1524**, 183–188.
Dittrich, S., Mitchell, S. L., Blagborough, A. M., Wang, Q., Wang, P., Sims, P. F. & Hyde, J. E. (2008). *Mol. Microbiol.* **67**, 609–618.
Emsley, P., Lohkamp, B., Scott, W. G. & Cowtan, K. (2010). *Acta Cryst.* D**66**, 486–501.
Hall, T. A. (1999). *Nucleic Acids Symp. Ser.* **41**, 91–98.
Holm, L. & Park, J. (2000). *Bioinformatics*, **16**, 566–567.
Holm, L. & Sander, C. (1995). *Trends Biochem. Sci.* **20**, 478–480.
Jones, T. A., Zou, J.-Y., Cowan, S. W. & Kjeldgaard, M. (1991). *Acta Cryst.* A**47**, 110–119.
Kang, D., Kim, S. & Yim, J. (1998). *Pteridines*, **9**, 69–84.
Kong, J. S., Kang, J.-Y., Kim, H. L., Kwon, O.-S., Lee, K. H. & Park, Y. S. (2006). *FEBS Lett.* **580**, 4900–4904.
Larkin, M. A., Blackshields, G., Brown, N. P., Chenna, R., McGettigan, P. A., McWilliam, H., Valentin, F., Wallace, I. M., Wilm, A., Lopez, R., Thompson, J. D., Gibson, T. J. & Higgins, D. G. (2007). *Bioinformatics*, **23**, 2947–2948.
Laskowski, R. A., MacArthur, M. W., Moss, D. S. & Thornton, J. M. (1993). *J. Appl. Cryst.* **26**, 283–291.
Lawrence, N. S., Pagels, M., Meredith, A., Jones, T. G., Hall, C. E., Pickles, C. S., Godfried, H. P., Banks, C. E., Compton, R. G. & Jiang, L. (2006). *Talanta*, **69**, 829–834.
Matsubara, M., Katoh, S., Akino, M. & Kaufman, S. (1966). *Biochim. Biophys. Acta*, **122**, 202–212.
McCarty, R. M., Somogyi, A. & Bandarian, V. (2009). *Biochemistry*, **48**, 2301–2303.
Murshudov, G. N., Skubák, P., Lebedev, A. A., Pannu, N. S., Steiner, R. A., Nicholls, R. A., Winn, M. D., Long, F. & Vagin, A. A. (2011). *Acta Cryst.* D**67**, 355–367.
Nagatsu, T. & Ichinose, H. (1999). *Mol. Neurobiol.* **19**, 79–96.
Nar, H., Huber, R., Heizmann, C. W., Thöny, B. & Bürgisser, D. (1994). *EMBO J.* **13**, 1255–1262.
Navaza, J. (1994). *Acta Cryst.* A**50**, 157–163.
Otwinowski, Z. & Minor, W. (1997). *Methods Enzymol.* **276**, 307–326.
Ploom, T., Thöny, B., Yim, J., Lee, S., Nar, H., Leimbacher, W., Richardson, J., Huber, R. & Auerbach, G. (1999). *J. Mol. Biol.* **286**, 851–860.
Pribat, A., Jeanguenin, L., Lara-Núñez, A., Ziemak, M. J., Hyde, J. E., de Crécy-Lagard, V. & Hanson, A. D. (2009). *J. Bacteriol.* **191**, 4158–4165.

Seo, K. H., Supangat, Kim, H. L., Park, Y. S., Jeon, C. O. & Lee, K. H. (2008). *Acta Cryst.* F**64**, 105–107.
Thöny, B., Auerbach, G. & Blau, N. (2000). *Biochem. J.* **347**, 1–16.
Vagin, A. & Teplyakov, A. (2010). *Acta Cryst.* D**66**, 22–25.
Wachi, Y., Burgess, J. G., Iwamoto, K., Yamada, N., Nakamura, N. & Matsunaga, T. (1995). *Biochim. Biophys. Acta*, **1244**, 165–168.
Winn, M. D. *et al.* (2011). *Acta Cryst.* D**67**, 235–242.
Woo, H. J., Hwang, Y. K., Kim, Y. J., Kang, J. Y., Choi, Y. K., Kim, C.-G. & Park, Y. S. (2002). *FEBS Lett.* **523**, 234–238.